



MIT Open Access Articles

Experimental study of gravitation effects in the flow of a particle-laden thin film on an inclined plane

The MIT Faculty has made this article openly available. **Please share** how this access benefits you. Your story matters.

Citation	Ward, Thomas et al. "Experimental Study of Gravitation Effects in the Flow of a Particle-laden Thin Film on an Inclined Plane." <i>Physics of Fluids</i> 21.8 (2009): 083305. © 2009 American Institute of Physics
As Published	http://dx.doi.org/10.1063/1.3208076
Publisher	American Institute of Physics (AIP)
Version	Final published version
Citable link	http://hdl.handle.net/1721.1/78571
Terms of Use	Article is made available in accordance with the publisher's policy and may be subject to US copyright law. Please refer to the publisher's site for terms of use.

Experimental study of gravitation effects in the flow of a particle-laden thin film on an inclined plane

Thomas Ward, Chi Wey, Robert Glidden, A. E. Hosoi, and A. L. Bertozzi

Citation: *Phys. Fluids* **21**, 083305 (2009); doi: 10.1063/1.3208076

View online: <http://dx.doi.org/10.1063/1.3208076>

View Table of Contents: <http://pof.aip.org/resource/1/PHFLE6/v21/i8>

Published by the [American Institute of Physics](#).

Additional information on Phys. Fluids

Journal Homepage: <http://pof.aip.org/>

Journal Information: http://pof.aip.org/about/about_the_journal

Top downloads: http://pof.aip.org/features/most_downloaded

Information for Authors: <http://pof.aip.org/authors>

ADVERTISEMENT



Running in Circles Looking for the Best Science Job?

Search hundreds of exciting
new jobs each month!

<http://careers.physicstoday.org/jobs>

physicstodayJOBS



Experimental study of gravitation effects in the flow of a particle-laden thin film on an inclined plane

Thomas Ward,^{1,a)} Chi Wey,^{2,b)} Robert Glidden,² A. E. Hosoi,³ and A. L. Bertozzi¹

¹Department of Mathematics, University of California, Los Angeles, California 90095-1555, USA

²Department of Mechanical and Aerospace Engineering, University of California, Los Angeles, California 90095-1597, USA

³Department of Mechanical Engineering, Hatsopoulos Microfluids Laboratory, Massachusetts Institute of Technology, 77 Massachusetts Avenue, Cambridge, Massachusetts 02139, USA

(Received 20 April 2009; accepted 29 July 2009; published online 20 August 2009)

The flow of viscous, particle-laden wetting thin films on an inclined plane is studied experimentally as the particle concentration is increased to the maximum packing limit. The slurry is a non-neutrally buoyant mixture of silicone oil and either solid glass beads or glass bubbles. At low concentrations ($\phi < 0.45$), the elapsed time versus average front position scales with the exponent predicted by Huppert [Nature (London) **300**, 427 (1982)]. At higher concentrations, the average front position still scales with the exponent predicted by Huppert on some time interval, but there are observable deviations due to internal motion of the particles. At the larger concentration values and at later times, the departure from Huppert is seen to strongly depend on total slurry volume V_T , inclination angle α , density difference, and particle size range. © 2009 American Institute of Physics. [DOI: 10.1063/1.3208076]

I. INTRODUCTION

Extensive research has been conducted on the flow of homogeneous thin films on inclined planes¹⁻⁴ and granular flows down inclined planes;⁵⁻⁸ however, relatively little research has been done in the intermediate regime of particle/fluid mixtures⁹⁻¹⁹ and, in particular, anisopycnic particle-laden thin film flows. Particle-laden fluid flow plays an important role in the dynamics of a variety of applications ranging from problems with large scales where gravity is important, such as mud slides and food processing, to blood flow, shaving creams (vapor-liquid slurries), and surface coating in which microscopic scales are relevant and gravity is negligible. Our goal is to present new experimental results for the bulk transport of a fixed volume of particle-laden thin fluid film propagating down an inclined plane.

Huppert¹ investigated the problem of a fixed volume of homogeneous Newtonian fluid flowing down an inclined plane using lubrication theory and continuity and neglecting surface tension and contact line effects along the propagating front. By solving a nonlinear partial differential equation for the conserved volume of a gravity-driven viscous liquid flowing down a plane, he found that the position of the propagating front, \hat{x}_N ($\hat{\cdot}$ denotes dimensional variables), is proportional to time to the one-third power, $\hat{t}^{1/3}$, or

$$\hat{x}_N = \left(\frac{\hat{t}}{\hat{C}_N} \right)^{1/3}, \quad (1)$$

where \hat{C}_N is a constant that depends on geometry and the material properties of the fluid. The theoretical model was compared with experimental data using homogeneous fluids on surfaces of varying inclination angle. Huppert found excellent agreement between the two despite the appearance of a fingering instability along the front. In this report we use Huppert's similarity solution, which is a shock solution for the average front position as a function of time, to compare flow characteristics of a particle-laden thin film of varying concentrations flowing down an inclined plane.

Consider a slurry consisting of an initially well-mixed solution of spherical glass beads of density ρ_S and radius R suspended in a viscous fluid of density ρ_L and absolute viscosity μ_L with the surrounding fluid a vapor of density ρ_V , see Fig. 1(a). The total slurry volume is $V_T = V_S + V_L$ and concentration $\phi = V_S / V_T$, where V_S and V_L are the volumes of the solid and liquid contents, respectively. The slurry has an average density $\bar{\rho}(\phi) = (1 - \phi)\rho_L + \phi\rho_S$ and is flowing due to gravity of magnitude g on a plane inclined at an angle α with respect to the horizontal. For initially well-mixed particle-laden thin films the concentration ϕ is constant. If Huppert's model holds on some interval of time for an initially well-mixed particle-laden thin film then a similarity solution exists where $\hat{C}_N = \hat{t} / \hat{x}_N^3$ is constant in time and the expression for the average front position of the propagating slurry is given by $x_N = C_N t^{1/3}$. The equations are made dimensionless by scaling \hat{x}_N by the track length L and time \hat{t} with the characteristic time $1/\omega$ where $\omega = 9\bar{\rho}gA^2 \sin \alpha / 4L^3 \mu_L$ and $A = V_T / w$ is the cross sectional area defined as the total slurry

^{a)}Present address: Department of Mechanical and Aerospace Engineering, North Carolina State University, 2601 Stinson Dr., Raleigh, NC 27695-7910.

^{b)}Present address: Department of Mechanical Engineering, Stanford University, Building 530, 440 Escondido Mall, Stanford, CA 94305-3030.

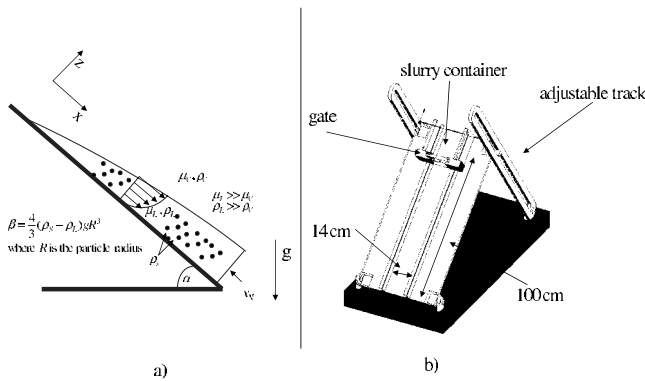


FIG. 1. (a) Problem schematic and (b) schematic of experimental setup.

volume divided by track width w . In dimensionless form Huppert's similarity solution constant is

$$C_N = \frac{9}{4\mu_L} \bar{\rho}(\phi) g A^2 \hat{C}_N \sin \alpha, \quad (2)$$

where this dimensionless constant C_N is unity for a homogeneous Newtonian fluid. Let $\beta = \frac{4}{3} \pi (\rho_S - \rho_L) g R^3$ be the internal buoyancy force parameter of a single particle where $\beta > 0$ denotes a systems where the particles in the slurry settle since they are heavier than the suspending fluid and $\beta < 0$ represents the opposite, i.e., a hard-sphere foam. Deviations from unity in the constant will be used to determine the influence of gravity on the thin film flow since it will strongly influence the dimensional constant \hat{C}_N .

In this paper we will perform experiments to compare an experimentally measured constant C_N of a particle-laden wetting thin film as a function of concentration, volume, and inclination angle to identify novel fluid behavior through observed trends in the data. The density of the glass beads in two sets of experiments are two and a half times that of the fluid ($\beta > 0$) and in the third set are one-tenth that of the fluid ($\beta < 0$). So one expects them to collect at the propagating front of the flowing slurry in some finite time due to gravitational settling¹¹ for the former and move in a direction opposite the propagating front in the latter. In Sec. III, we will also qualitatively compare images of the propagating front to determine if there is any relationship between the appearance of the particle rich capillary ridge and noncontinuum behavior, and in Sec. IV we compare the results for various experiments and offer suggestions for the observed trends.

II. EXPERIMENTS: MATERIALS, PROCEDURES, AND PHYSICAL SCALES

Three sets of experiments are performed, two using solid glass spheres but with slightly different mixing protocols and the third with glass bubbles. In one set of solid sphere experiments called experiment A, the parameters that were varied are the particle size range (either 106–180 or 250–425 μm in diameter), volume ($50 \text{ ml} < V_T < 130 \text{ ml}$), tilt angle (35° , 45° , or 55°), and concentration (0, 0.35, 0.45, 0.50, or 0.55) with the resulting data averaged over the concentration for a given particle size. The fluid viscosity in

TABLE I. List of experiments performed to determine gravity effects in flowing particle-laden thin films. The density of the glass spheres used in experiments A and B is $\rho_S = 2.5 \text{ g/cm}^3$ and the density of the hollow glass spheres used in experiment C is $\rho_S = 0.15 \text{ g/cm}^3$. The concentration range, ϕ , in experiment B is in increments of 0.01. Slurry volumes of approximately 50–130 ml are used in experiment A, 50–70 ml in experiment B, and 30 ml in experiment C.

Particle size (μm)	Tilt angles (deg)	Concentrations (V/V_T)	Fluid viscosity (cSt)
Experiment A			
106–180	35, 45, 55	0, 0.35, 0.45, 0.50, 0.55	1000
250–425	35, 45, 55	0.35, 0.45, 0.50, 0.55	1000
Experiment B			
106–180	55, 60, 65, 75	0.50–0.56	100, 500, 1000
250–425	55, 60, 65, 75	0.50–0.56	1000, 5000, 10 000
450–800	55, 60, 65, 75	0.50–0.56	5000, 10 000
Experiment C			
10	35, 45, 55	0.35, 0.45, 0.55	10, 50, 100

these experiments were fixed at $\mu_L = 1000$ cSt. In the second set of experiments called experiment B, the particle size range (106–180, 250–425, or 450–800 μm), concentration (0.50, 0.51, 0.52, 0.53, 0.54, 0.55, or 0.56), tilt angle (55° , 60° , 65° , or 75°), volume ($50 \text{ ml} < V_T < 70 \text{ ml}$), and background fluid viscosity were the varied parameters with the resulting viscosity data, once again averaged over the concentration for a given particle size. The viscosities were varied depending on particle size with $\mu_L = 100, 500, \text{ or } 1000$ cSt for the 106–180 μm particles, $\mu_L = 1000, 5000, \text{ or } 10 000$ for the 250–425 μm particles, and $\mu_L = 5000$ or 10 000 for the 450–800 μm particles. The viscosities were chosen so that the particle velocity based on settling is approximately the same for each experiment. Experiment A was performed over a wider range of concentration so it may be more useful in determining global trends while experiment B is done in the limit $\phi \rightarrow \phi_{\text{max}}$ to determine behavior as the system begins to phase separate. Test runs in experiment C were performed using glass bubbles of a single size with a fixed total volume of approximately $V_T = 30 \text{ ml}$ while varying the concentration, at either 0.35, 0.45, or 0.55, and background viscosity, at either 10, 50, or 100 cSt, and averaged over tilt angles of either 35° , 45° , or 55° . A summary of the parameters that were varied during the experiments is shown in Table I. Since we are averaging over some parameter each experimental run is performed once.

The suspending fluids used were silicone oil (Clearco Products) for each experiment. Each silicone oil fluid had a density of approximately 0.96 g/cm^3 . Soda-lime glass beads (Ceroglass) with a density of approximately 2.5 g/cm^3 were used in experiments A and B while hollow glass spheres (3M) with a density of 0.15 g/cm^3 and diameter of approximately $10 \mu\text{m}$ were used in experiment C. These densities gave buoyancy force values of approximately $\beta = 0.0027, 0.0214, \text{ and } 0.170$ dynes for the 106–180, 250–425, or 450–800 μm particles (based on average) used in experiments A and B and $\beta = -3.5 \times 10^{-6}$ dynes for the $10 \mu\text{m}$

particles used in experiment C. Silicone oils are good thermal insulators so we do not expect much deviation in the viscosity for small variations in the room temperature.

The experimental apparatus consists of a 100 cm long, 50 cm wide, acrylic sheet with a track approximately $w=14$ cm in width. The side walls of the track are approximately 1–2 cm high which is much larger than the film thickness so the fluid cannot spill over. The slurry's cross sectional areas were constant at 2 and 4 cm² in experiments C and B, respectively. These values are $4 \text{ cm}^2 < A < 9 \text{ cm}^2$ for experiment A, which are similar to those used by Huppert.¹ The acrylic sheet is mounted to an adjustable stand capable of inclination angles ranging from 5° to 80°. Near the top of the acrylic sheet is a gated reservoir from which we release a finite volume of mixture. A schematic of the experimental setup is shown in Fig. 1(b). We estimate the time constant, $1/\omega$, which can be interpreted as a residence time, to be in the range of $100 \text{ s} < \hat{t} < 1000 \text{ s}$ using values for our physical parameters.

A. Mixing protocol: Experiments A and C

The slurry materials are placed in a large horizontally oriented jar and slowly rotated for several hours until the particles are uniformly suspended in the fluid, creating a well-mixed slurry. The particles can settle out fairly quickly so the experiments were performed immediately after the slurry was well mixed. To determine ϕ_{\max} for $\beta > 0$, known volumes of fluid and beads were mixed and placed in a graduated cylinder. The maximum packing fraction can be estimated from the excess liquid volume fraction. The value of ϕ_{\max} is measured to be approximately 0.57–0.58 which is within 10% of the theoretically predicted value of 0.64 for monodisperse hard spheres. While our system is not monodisperse the deviation in particle size is much smaller than their average in both particle size ranges studied. The values of concentration used in this experiment were $\phi=0, 0.35, 0.45, 0.50,$ and 0.55 .

B. Mixing protocol: Experiment B

Here the slurry materials are placed in a plastic cup and slowly mixed by hand until the slurry becomes uniform. Slow mixing is needed to avoid generating air bubbles which changes the viscosity. This process is more efficient for slurry mixing when a very viscous background liquid is used. Since the settling velocity is inversely proportional to the background fluid viscosity we can increase the particle size for the larger viscosity fluids.

1. Procedure

A known volume of the slurry is extracted with a plastic syringe, modified to entrain a large volume of the viscous slurry solution. A camera positioned vertically above the track takes still images at predetermined time intervals. The images are then analyzed via MATLAB and an average front position is calculated for each image. Images are converted to gray scale and sharp contrasts are traced using a function included in the image processing toolbox. After the edges have been traced, the resulting image is filtered to ensure that

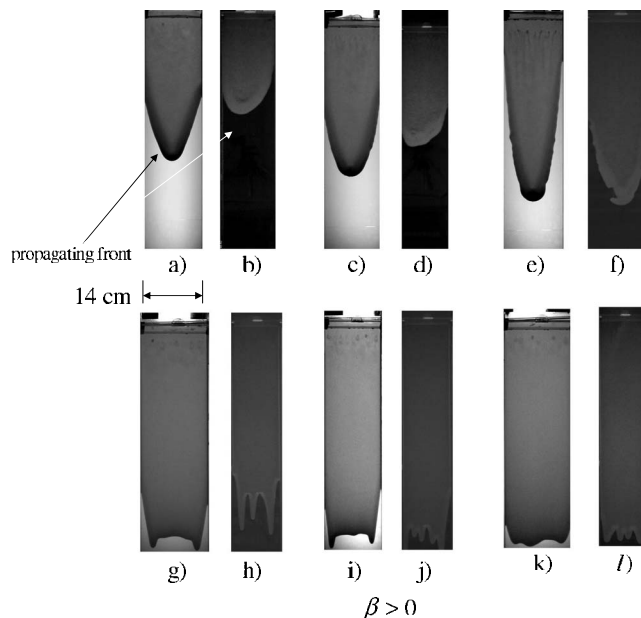


FIG. 2. Static images from 12 experimental trials (experiment A) of flowing slurries for particle sizes [(a), (c), (e), (g), (i), and (k)] 106–180 μm ($\beta=0.0027$ dynes) and [(b), (d), (f), (h), (j), and (l)] 250–425 μm ($\beta=0.0214$ dynes). The top row of images (a)–(f) shows the propagating front for a 0.55 concentration and volume of 70 ml with inclination angles $\alpha=[(a) \text{ and } (b)] 35^\circ$, [(c) and (d)] 45° , and [(e) and (f)] 55° . The bottom row of images (g)–(l) shows the propagating front for concentration of $\phi=0.35$, inclination angle of 40° , and volumes of [(g) and (h)] 70 ml, [(i) and (j)] 90 ml, and [(k) and (l)] 110 ml. The images are taken at dimensional times of $\hat{t}=(a) 1450 \text{ s}$, (b) 724 s, (c) 1485 s, (d) 945 s, (e) 1288 s, (f) 542 s, (g) 273 s, (h) 590 s, (i) 238 s, (j) 332 s, (k) 130 s, and (l) 256 s.

only the traced fluid front remains. An averaged front position, averaged over some 200 data points, in pixels (relative to the gate opening) is calculated and later converted into a physical distance.

III. EXPERIMENTAL RESULTS

A. Qualitative observations

1. $\beta > 0$

Figure 2 shows still images from experiment A ($\beta > 0$) of the flowing slurry, with particle diameters of either 250–425 μm in Figs. 2(b), 2(d), 2(f), 2(j), 2(h), and 2(l) (dark background) or 106–180 μm in Figs. 2(a), 2(c), 2(e), 2(g), 2(i), and 2(k) (light background) (450–800 μm diameter data for experiment B is analogous) at times indicated in the caption. The first series of images, Figs. 2(a)–2(f), shows the propagating front for a fixed concentration of $\phi=0.55$ and volume of 70 ml while the tilt angle is 35° , 45° , or 55° as indicated in the caption. In general, as the tilt angle increases the propagating front begins to coarsen along the single finger and resembles a slug. In Fig. 2(f), as the particles begin to collect near the propagating front, the higher particle concentration region begins to move faster than the rest of the slurry and the system exhibits noncontinuum behavior and phase separates as the heavier front begins to break off. At higher inclination angles ($>55^\circ$) the front completely detaches from the bulk of the flowing material.

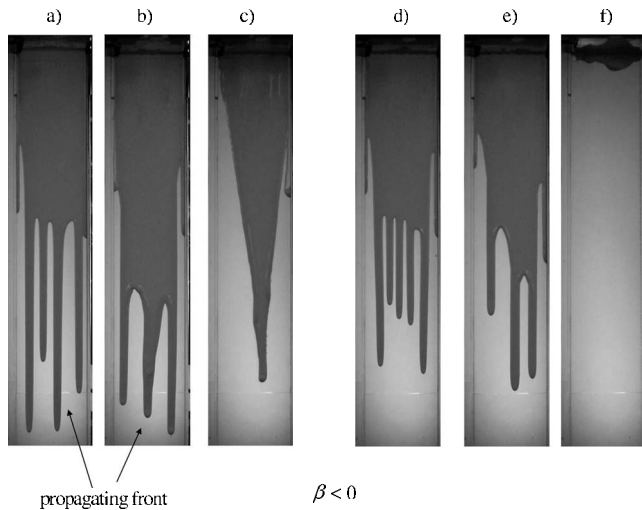


FIG. 3. Static images from six experimental trials from experiment C ($\beta = -3.5 \times 10^{-6}$ dynes) of flowing slurries with tilt angle $\alpha = 45^\circ$ for buoyant particles with background fluid viscosity of either [(a)–(c)] 10 or [(d)–(f)] 100 cSt as indicated with concentrations $\phi = [(a) \text{ and } (d)] 0.35$, [(b) and (e)] 0.45, and [(c) and (f)] 0.55. The images are taken at dimensional times of $t = (a) 30$ s, (b) 180 s, (c) 550 s, (d) 230 s, (e) 875 s, and (f) 944 s.

Figures 2(g)–2(l) show the propagating slurry front at an inclination angle of 40° and concentration of 0.35 as the volume is increased from 70 to 110 ml. In Figs. 2(g) and 2(i), the usual fingering instability is apparent and nearly symmetric at the volumes shown. The same trends are observed for the larger beads as well in Figs. 2(h) and 2(j). It also appears that the fingering is suppressed as the volume is increased in Figs. 2(k) and 2(l) where the fluid has flowed nearly the complete length of the track. Also, the finger lengths are much shorter than those of the smaller volumes flowing under similar conditions shown in the previous panels.

2. $\beta < 0$

Figure 3 shows still images from experiment C ($\beta < 0$) at times indicated in the caption. Figure 3 shows the propagating front at an inclination angle of 45° and volume of $V_T = 30$ ml. In Figs. 3(a)–3(c) the concentration varies from 0.35 to 0.45 to 0.55, respectively, while the background fluid viscosity is fixed at 10 cSt, representing the lowest viscosity fluid used in all of the experiments, A, B, or C. In Fig. 3(a), with $\phi = 0.35$, the propagating front exhibits a fingering instability characterized by a wide separation of the regions of positive and negative curvatures. Because of this wide separation the average front position is a relatively shorter distance from the gate than in the $\beta > 0$ experiments. A similar fingering pattern is seen in Fig. 3(b), with $\phi = 0.45$, although the number of fingers is smaller and the average front distance traveled is farther than in the $\phi = 0.35$ experiment. Figure 3(c) shows the propagating front for the largest concentration used with the 10 cSt fluid at 45° . Here the fingering instability is represented by a single finger extended from the gate and moving down the center of the track. Part of this motion is due to the fact that as the lighter particles begin to move upward they create a fluid rich region below. The vol-

ume of fluid in the particle rich region increases over time until a layer of clear liquid is created and this flows down the track. For the lighter viscosity fluids, this separated stream can carry some of the low-density particles plus fluid with it. Note that while the propagating front appears relatively far from the reservoir at the top of the panel due to the fingering phenomenon, the average front position is still relatively close to the gate.

Figures 3(d)–3(f) show still images for concentrations of 0.35, 0.45, and 0.55, respectively, with a background fluid viscosity of 100 cSt. Figure 3(d) shows a fingering instability along the propagating front that strongly resembles in length and number the fingers seen in Fig. 3(a). The only noticeable difference is that in Fig. 3(d) an estimate for the average front position (measured near the finger troughs) is slightly farther from the reservoir than what is shown in Fig. 3(a). Figure 3(e) is not discernibly different from the experiment with similar parameters shown in Fig. 3(b). But Fig. 3(f) is clearly different than the other $\phi = 0.55$ experiment shown in Fig. 3(c). In Fig. 3(f) the slurry barely leaves the gate and does not travel one track width suggesting that the flow may not be fully developed. While the same separation process occurred in the lower background viscosity experiment shown in Fig. 3(c), the end results are very different. So while both particle rich regions in Figs. 3(c) and 3(f) are approaching $\phi \rightarrow \phi_{\max}$, the experiment with the high background viscosity is more resistant to gravity because of the internal dynamics of the particle rich region.

B. Quantitative measurements

The qualitative trends suggest that the presence of particles greatly affects the geometry of the propagating front. However, the measured average position \hat{x}_N versus time, still shows self-similar behavior, i.e., similar to that measured by Huppert.¹ To better understand this phenomenon we experimentally vary the following parameters: buoyancy parameter β , volume V_T , particle concentration ϕ , inclination angle α , and background fluid viscosity μ_L , over a wide range of parameters.

Figure 4 shows plots of average front positions from experiment A, \hat{x}_N versus $t^{1/3}$, for inclination angles $\alpha = (a) 35^\circ$, (b) 45° , and (c) 55° , with fixed concentrations of $\phi = 0, 0.35, 0.45$, and 0.55 and fixed volumes of 20 and 70 ml for the homogeneous and particle-laden fluids, respectively. The flow clearly has some initial transient behavior that seems to grow with the concentration. After this initial transient the particle-laden thin film begins to accelerate. In Fig. 4, at the highest concentration, $\phi = 0.55$, the flow takes approximately 27 s to become fully developed and at the lowest concentration, $\phi = 0.35$, it takes less than 1 s. The plots appear linear with the $t^{1/3}$ scaling in the fully developed region, with linear behavior over at least two decades of time. Note that in Fig. 4 not all are straight lines especially in the limit $\phi \rightarrow \phi_{\max}$. Nevertheless, there is a domain of those lines which indicate a timescale of the flow. We will use this time interval to determine a parameter \hat{C}_N for the particular flow.

Figure 5 shows plots of average front positions from experiment C, \hat{x}_N versus $t^{1/3}$, for an inclination angle of

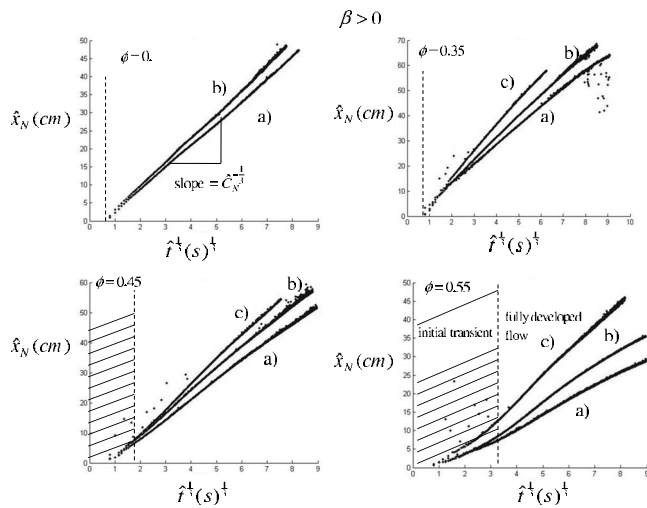


FIG. 4. Plots of average front position \hat{x}_N vs $\hat{t}^{1/3}$ for a 250–425 μm ($\beta=0.0214$ dynes) glass bead slurry mixture. The tilt angles are $\alpha=(a)$ 35°, (b) 45°, and (c) 55°. These data were used to measure the slopes which contain information for \hat{C}_N . Note that we do not expect the data to collapse onto one line; rather we expect to see a linear relationship between \hat{x}_N and $\hat{t}^{1/3}$ after the initial transients have decayed. The variation at each concentration is due to the difference in inclination angle and/or volume for each experiment. The vertical dashed line roughly indicates the transition from transient to fully developed flow. There are no lines drawn through the data point and no fitting parameters.

$\alpha=45^\circ$, with fixed concentrations of $\phi=(a)$ 0.35, (b) 0.45, and (c) 0.55 with background fluid viscosities as indicated on the graph. Once again, each of the plots exhibits characteristics of the flow suggesting some initial transient behavior but the correlation with increasing concentration is not so clear. One noticeable trend in the initial transients for the $\beta < 0$ experimental results is that they seem to be independent of concentration. Part of the inability to correlate the initial transient with concentration is due to the speed of the film as it leaves the gate. With a low background fluid viscosity, and the film initially *thick*, then the initial speed is relatively fast compared to later times (the velocity from the

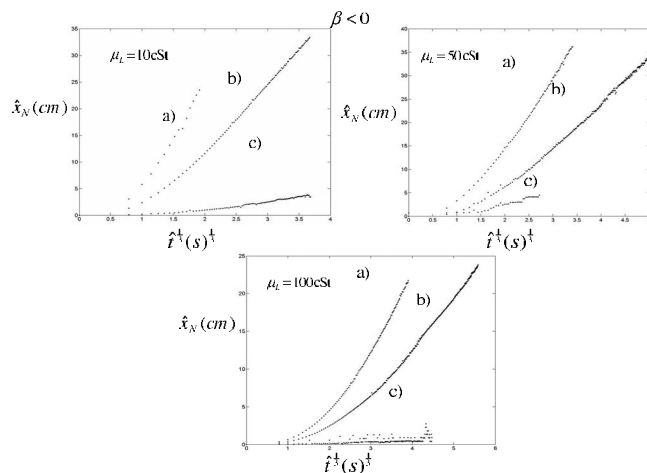


FIG. 5. Plots of average front position \hat{x}_N vs $\hat{t}^{1/3}$ for a buoyant glass sphere slurry mixture ($\beta=-3.5 \times 10^{-6}$ dynes). The tilt angle is $\alpha=45^\circ$ with $\phi=(a)$ 0.35, (b) 0.45, and (c) 0.55. There are no lines drawn through the data point and no fitting parameters.

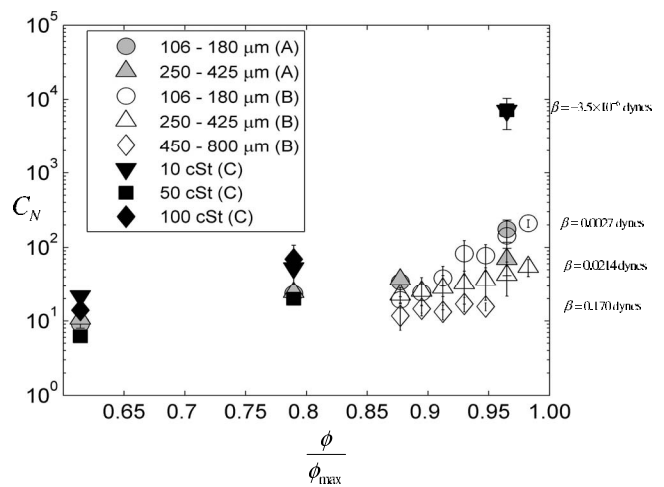


FIG. 6. Plot of dimensionless constant C_N vs scaled concentration ϕ/ϕ_{max} for experiments A–C (shown in parenthesis). The shaded symbols correspond to experiment A with particle sizes (a) (○) 106–180 μm and (△) 250–425 μm glass bead slurry mixtures. The open symbols correspond to experiment B with particle sizes (○) 106–180 μm , (△) 250–425 μm , and (◇) 450–800 μm . Experiments A and B correspond to data sets for $\beta > 0$ as indicated on the right. The filled symbols correspond to experiment C, where $\beta=-3.5 \times 10^{-6}$ dynes, i.e., the particles are lighter than the suspending fluid. The particles size is constant ($\approx 10 \mu\text{m}$) with background fluid viscosities of (▼) 10 cSt, (■) 50 cSt, and (◆) 100 cSt. No fitting parameters are used in producing data for this figure.

Huppert solution is singular at $\hat{t}=0$). So the lower viscosity fluids actually have lower temporal resolution than their higher background viscosity counterparts. This can also be seen in Fig. 4 for the 10 cSt fluid with $\phi=0.35$. The spacing between points is much farther than in any of the other experiments because of the fluid speed. But after the initial transient it appears that the front moves linearly with time to the one-third power as predicted by the Huppert solution. In the largest concentration and largest background fluid viscosity experiment, Fig. 5(c) bottom panel, we see that the slurry does not move at least one width of the track so we assume that this experiment is not fully developed. We do not include this result in the comparison with the correlation but report the result because it may be of interest. The slopes for each of the data curves in either experiment yield the information necessary to calculate the constant C_N .

C. Quantitative comparisons

Figure 6 shows plots of the measured constant C_N versus ϕ/ϕ_{max} , with C_N as defined in Eq. (2), for experiments A (shaded symbols), B (open symbols), and C (filled symbols). The error bars in Fig. 6 represent the standard deviation that is due to variations in the measured constant value due to the inclination angle α and volume \hat{V}_T while averaged over concentration in experiment A, while the bars for experiment B represent deviations in the measured constant value due to changes in the background fluid viscosity and tilt angle while averaged over concentration. Experiments A and B both represent data with value $\beta > 0$ where the particles are heavier than the suspending fluid. The data points for experiment C shown in Fig. 6 are averaged over concentration while vary-

ing the tilt angle for fixed total slurry volume and suspending fluid viscosity with $\beta < 0$, so the hollow glass spheres are lighter than the suspending fluid.

The data points in Fig. 6 for experiment A represent the four concentrations 0.35, 0.45, 0.5, or 0.55 for either the 106–180 or 250–425 μm particle size distributions. For most of the data for a given particle size, the standard deviation is less than the symbol size but increases with increasing concentration, indicating that the variation due to volume and angle becomes more significant. For low concentrations, $< 45\%$, the standard deviation in the measured constant values are relatively small for either particle size. At larger concentrations, $> 45\%$, the measured constant has a larger standard deviation. This trend is true in either set of experiments using the 106–180 or 250–425 μm diameter particles. The measured constants C_N are nearly identical for both bead sizes up until a concentration of 0.50.

In experiment B the focus is on the constant as we approach the maximum packing limit for the three solid particle sizes with $\beta = 0.0027, 0.0214, \text{ or } 0.170$ dynes. This set of data represents a more detailed interpretation of the data shown from experiment A. The data for the three particle sizes shown for experiment B overlap at lower concentration of $\phi \approx 0.50$. At the higher concentrations the data suggest that there is a separation of times for the three particles sizes. The smaller particles, 106–180 μm , have a constant that is larger in value than in the other experiments. As the particles size is increased to 250–425 μm the measured constant is slightly lower in value than in the smaller particle case at the larger concentrations. As the size is increased to the largest particles studied, 450–800 μm , again there is a decrease in the measured constant when compared with the other experiments. In fact, the last two experiments at $\phi = 0.55$ and 0.56 are not shown because the constant could not be accurately measured. This is because the slurry breaks up and slides down the track like a solid.

Figure 6 also shows results for the hollow glass spheres from experiment C, $\beta = -3.5 \times 10^{-6}$ dynes, averaged over tilt angle α for varying background fluid viscosity. The three sets of data are plotted at the same concentrations of $\phi = 0.35, 0.45, \text{ or } 0.55$ as in the experiment A data. Note that the hollow glass spheres' maximum packing is more difficult to measure because the particles may not stay immersed in the fluid as they begin to form a particle rich cake at the top in a batch sedimentation experiment. This value though is within 10% of the theoretical value so it is a good estimate. For the 10 and 50 cSt fluids at $\phi = 0.55$ the deviation is larger than that of the same fluids at $\phi = 0.45$. Overall the deviation in the measured constant is less than one order of magnitude at the largest concentration shown but the absolute values for the constants are at least two orders of magnitude larger than in the heavy particle experiments (A and B).

IV. DISCUSSION AND CONCLUSION

From the experimental data presented there are some general trends that are similar in each experiment regardless of the sign of the buoyancy force value β . The first is that the constant C_N is greater than unity in all experimental results

shown. Other trends are seen when comparing constant values at the lower concentrations $\phi = 0.35$ and 0.45 where the data in each of the experiments (A, B, and C) seem to collapse to nearly a single value. This is a semilogarithmic plot so there is more separation in the measured constants in this range than what the plot shows, but when compared to the data at larger concentration values, the constants at lower concentrations are relatively closer in value. The images shown in Figs. 2 and 3 also suggest that the propagating front morphologies are also similar with multiple fingers at low concentrations [Figs. 2(g)–2(l) and Figs. 3(a) and 3(d)] and single fingers resembling a slug at the higher concentrations [Figs. 2(a)–2(f) and Figs. 3(c) and 3(f)].

The constants produced as $\phi \rightarrow \phi_{\text{max}}$ appear to diverge in each experiment but diverge much more rapidly as the concentration is increased in experiment C. This suggest that there may be separation of the time scales in experiment A, B, or C as the concentration is increased to the maximum packing limit. The only difference between the two sets of experiments (A and B or C) is the direction of the buoyancy force value β where it is positive in experiments A and B and negative for experiment C. The rest of this discussion focuses on how the results of experiments A and B differ from those of experiment C and possible reasons based on the experimental results.

For most experiments performed for experiment A in our parameter ranges, $35^\circ < \alpha < 55^\circ$ and $0.35 < \phi < 0.55$, the change in constant C_N as the parameters are varied is smooth, an observation that is supported by the data in Fig. 6. The same trends are seen in experiment B where the change in concentration is more gradual. The decrease in measured constant for larger particles that is seen in either experiment A or B, i.e., as the buoyancy force value β is increased, may be attributed to the fact that a relatively heavier propagating front could generate a faster moving leading edge. This is clearly seen in Fig. 6 when comparing the 106–180 and 450–800 μm particles at $\phi = 0.55$ from experiment B. This is also seen in comparing the elapsed times for the two images shown in Figs. 2(e) and 2(f), where the inclination angle, volume, and concentration are identical but the particles sizes are 106–180 and 250–425 μm , respectively. The distance the slurry travels is nearly identical in the images for these two experiments, and when comparing the elapsed time required to reach this distance in each experiment, which is 1288 and 542 s for Figs. 2(e) and 2(f), respectively, we see that it takes about one-half the time for the slurry with the larger particles, i.e., the larger buoyancy force. We see that this idea is indeed consistent with Eq. (1), where an increase in speed of the front \dot{x}_N over a fixed time interval $\Delta \hat{t} = \hat{t} - \hat{t}_0$ would lead to a lower constant value when compared to a slower moving fluid over the same interval.

For experiment C, where $\beta = -3.5 \times 10^{-6}$ dynes, i.e., < 0 , the trends seen in the heavy particle experiments, A and B, where $\beta > 0$, are not observed. Here the lighter particles tend to slow down the propagating front leading to a relatively higher constant value, where the value at the largest concentration in experiment C, $\phi = 0.55$, is almost two orders of magnitude greater than in experiments A and B (see Fig. 6). This is also seen when comparing the elapsed times for

the two experiments, where the time required to travel the distance shown in Fig. 3(f) is almost as long as the time required for any of the experiments shown in Fig. 2. This is surprising because the background fluid viscosities used for the experimental results shown in Fig. 2 are at least one order of magnitude less than in any of the A or B experiments. The difference between the heavy and lighter particle experiments is the direction of the particle buoyancy force relative to that of the suspending fluid. Since the buoyancy force within the total volume of slurry opposes gravity in the lighter particle experiments, it is also opposing gravity acting on the total volume that is pulling it downward. This is because while the lighter particles are buoyant in the fluid, the mixture is not lighter than the surround air, or $\rho_L > \rho_S > \rho_V$. So this phenomenon produces a solid hard-sphere foam that has a measured constant which appears to diverge much faster than in the heavy particle experiments where $\beta > 0$, even though the value for β in experiment C is measured in microdynes or the absolute value is about three orders of magnitude less than in experiments A and B.

In conclusion the scaling from the Huppert solutions still appears to be useful in characterizing these types of bulk fluid flow problems. Alternatively, a shock theory has already been developed for constant flux slurries.²⁰ An analogous theory for the constant volume problem would require a model involving rarefaction-shock solutions which is outside the scope of this experimental paper but is also of interest.

ACKNOWLEDGMENTS

We thank H. E. Huppert for his useful comments. We also would like to thank Ben Cook for many useful conversations. T.W. would like to acknowledge that support for this work was provided by the NSF-VIGRE program (Grant No. DMS-0502315). Additional support was provided by NSF Grant Nos. DMS-0601395, DMS-0244498, ACI-0321917, and ACI-0323672 and by ONR Grant No. N000140410078.

- ¹H. E. Huppert, "Flow and instability of a viscous current down a slope," *Nature (London)* **300**, 427 (1982).
- ²M. F. G. Johnson, R. A. Schluter, M. J. Miksis, and S. G. Bankoff, "Experimental study of rivulet formation on an inclined plate by fluorescent imaging," *J. Fluid Mech.* **394**, 339 (1999).
- ³A. Oron, S. H. Davis, and S. G. Bankoff, "Long-scale evolution of thin liquid films," *Rev. Mod. Phys.* **69**, 931 (1997).
- ⁴J. Sur, A. L. Bertozzi, and R. P. Behringer, "Reverse undercompressive shock structures in driven thin film flow," *Phys. Rev. Lett.* **90**, 126105 (2003).
- ⁵C. Cassar, M. Nicolas, and O. Pouliquen, "Submarine granular flows down inclined planes," *Phys. Fluids* **17**, 103301 (2005).
- ⁶O. Pouliquen, "Scaling laws in granular flows down rough inclined planes," *Phys. Fluids* **11**, 542 (1999).
- ⁷O. Pouliquen, J. Delous, and S. B. Savage, "Fingering in granular flows," *Nature (London)* **386**, 816 (1997).
- ⁸H. E. Huppert, "Quantitative modelling of granular suspension flows," *Philos. Trans. R. Soc. London, Ser. A* **356**, 2471 (1998).
- ⁹B. D. Timberlake and J. M. Morris, "Particle migration and free-surface topography in inclined plane flow of a suspension," *J. Fluid Mech.* **538**, 309 (2005).
- ¹⁰J. D. Parsons, K. X. Whipple, and A. Simoni, "Experimental study of the grain-flow, fluid-mud transition in debris flows," *J. Geol.* **109**, 427 (2001).
- ¹¹J. Zhou, B. Dupuy, A. L. Bertozzi, and A. E. Hosoi, "Theory for shock dynamics in particle-laden thin films," *Phys. Rev. Lett.* **94**, 117803 (2005).
- ¹²D. Leighton and A. Acrivos, "Viscous resuspension," *Chem. Eng. Sci.* **41**, 1377 (1986).
- ¹³D. Leighton and A. Acrivos, "The shear-induced migration of particles in concentrated suspensions," *J. Fluid Mech.* **181**, 415 (1987).
- ¹⁴J. F. Morris and J. F. Brady, "Pressure-driven flow of a suspension: Buoyancy effects," *Int. J. Multiphase Flow* **24**, 105 (1998).
- ¹⁵R. Rao, L. Mondy, A. Sun, and S. Altobelli, "A numerical and experimental study of batch sedimentation and viscous resuspension," *Int. J. Numer. Methods Fluids* **39**, 465 (2002).
- ¹⁶J. T. Norman, H. V. Nayak, and R. T. Bonnecaze, "Migration of buoyant particles in low-Reynolds-number pressure-driven flows," *J. Fluid Mech.* **523**, 1 (2005).
- ¹⁷A. Acrivos and E. Herbolzheimer, "Enhanced sedimentation in settling tanks with inclined walls," *J. Fluid Mech.* **92**, 435 (1979).
- ¹⁸E. Herbolzheimer and A. Acrivos, "Enhanced sedimentation in narrow tilted channels," *J. Fluid Mech.* **108**, 485 (1981).
- ¹⁹C. Mouquet, V. Greffeuille, and S. Treche, "Characterization of the consistency of gruels consumed by infants in developing countries: Assessment of the Bostwick consistometer and comparison with viscosity measurements and sensory perception," *Int. J. Food Sci. Nutr.* **57**, 459 (2006).
- ²⁰B. Cook, A. L. Bertozzi, and A. E. Hosoi, "Shock solutions for particle-laden thin films," *SIAM J. Appl. Math.* **68**, 760 (2008).